Inorganic Chemistry

Article

pubs.acs.org/IC

Luminescent Dirhenium(I)-Double-Heterostranded Helicate and Mesocate

Bhaskaran Shankar,[†] Saugata Sahu,[‡] Naina Deibel,[§] David Schweinfurth,[§,∥] Biprajit Sarkar,[§,∥] Palani Elumalai,[†] Deepak Gupta,[†] Firasat Hussain,[†] Govindarajan Krishnamoorthy,[‡] and Malaichamy Sathiyendiran*[,†]

[†]Department of Chemistry, University of Delhi, Delhi 110 007, India

[‡]Department of Chemistry, Indian Institute of Technology Guwahati, Guwahati 781 039, India

[§]Institut für Anorganische Chemie, Universität Stuttgart, Pfaffenwaldring 55, D-70550 Stuttgart, Germany

[∥]Institut für Chemie und Biochemie, Anorganische Chemie, Freie Universität Berlin, Fabeckstraße 34-36, D-14195 Berlin, Germany

Supporting Information

ABSTRACT: The semirigid ligands 1,4-bis(2-(2-hydroxyphenyl)benzimidazol-1-ylmethyl)benzene (H_2-pBC) and 1,3-bis(2-(2-hydroxyphenyl)benzimidazol-1-ylmethyl)-2,4,6-trimethylbenzene (H_2-mBC), containing two hydroxyphenylbenzimidazolyl units as bis-chelating (or bis-(bidentate)) N∩OH donor, were synthesized and were used to assemble neutral, luminescent heteroleptic, unsaturated double-hetero-stranded, rhenium(I)-based helicate (**1**) and mesocate (**2**) with the flexible bis(monodentate) nitrogen donor (1,4-bis(benzimidazol-1-ylmethyl)benzene/1,3-bis-(benzimidazol-1-ylmethyl)benzene), and $Re_2(CO)_{10}$. The photophysical properties of the complexes were studied. Both complexes **1** and **2** exhibit dual emissions in both solution and solid state. In solution, these complexes show both fluorescence and phosphorescence. Complex **1** undergoes a predominantly ligand-centered oxidation, resulting in the generation of phenoxyl radicals.

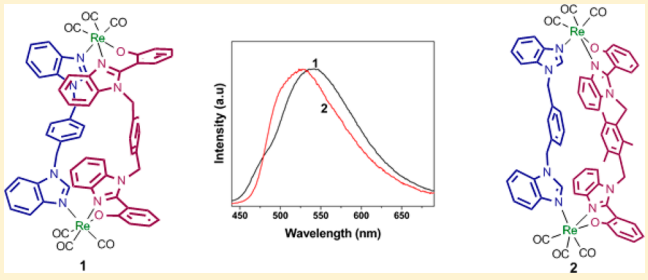

INTRODUCTION

The design and synthesis of metallocycles for use in functional applications such as molecular sensors, catalysts, dye-sensitized solar-cells, electroluminescent devices, and biomolecular imaging have attracted considerable attention.[1] One class of metallocycles, namely rhenium(I)-based complexes consisting of *fac*-$Re(CO)_3$, and an imine with/without additional donors, displayed interesting photophysical and electrochemical properties.[2−5] Because of the stability and intrinsic properties of these complexes, efforts are being directed toward the synthesis of new metallocycles. Over the past 15 years, much attention has focused on using only a few types of building blocks for rhenium(I)-based metallocycles. For example, neutral donors have been limited to rigid/flexible ligands containing pyridyl, imidazolyl, and benzimidazolyl units. RX^- (X = O/S; R = H, alkyl, aryl), biimidazole, bibenzimidazole, 2,2′-bipyrimidine, indigo, and hydroxybenzoquinone derivatives have been used as rigid anionic donors.[2−5] Few complexes containing bispyridylpyridone and 3-hydroxy-1,2,3-benzotriazine are known.[6] It is now well documented that the *fac*-$Re(CO)_3$ core needs neutral ditopic/tritopic/polytopic ligands with neutral two-electron-coordinating donors and two μ_2-XR bridging donor/dianionic bis-chelating ligands with three-electron-chelating donors to assemble rhenium(I)-based metallocycles (Figure 1), but donors other than the above-mentioned building blocks are rarely use. In continuation of our recent work on the synthesis of rhenium(I)-based metallocycles from flexible ligands,[5] we propose that introducing a hydroxyl or phenolic unit adjacent to the neutral nitrogen donor would lead to a new type of chelating ligand, resulting in metallocycles consisting of *fac*-$Re(CO)_3$, neutral flexible nitrogen donors, and anionic flexible N∩O donors.

Herein, a new type of neutral, flexible bis-chelating N∩OH donors (1,4-bis(2-(2-hydroxyphenyl)benzimidazol-1-ylmethyl)-benzene (H_2-pBC) and 1,3-bis(2-(2-hydroxyphenyl)-benzimidazol-1-ylmethyl)2,4,6-trimethylbenzene (H_2-mBC), Figure 1) and their rhenium(I)-based helicate (**1**) and mesocate (**2**) are reported. Self-assembly of the helicate and mesocate was achieved using $Re_2(CO)_{10}$, flexible bis-chelating (or bis(bidentate)) H_2-pBC/H_2-mBC N∩OH donors, and bis(monodentate) nitrogen donors in a one-step process. The ligands and complexes were characterized by elemental analysis, ESI-MS, FT-IR, and ^{1}H NMR spectroscopy. The molecular structures of ligands were deduced from DFT calculations, and complexes were confirmed by single-crystal X-ray crystallography. The photophysical and electrochemical properties of complexes were studied using various techniques.

Received: September 12, 2013
Published: January 6, 2014

 © 2014 American Chemical Society dx.doi.org/10.1021/ic4023135 | *Inorg. Chem.* 2014, 53, 922−930

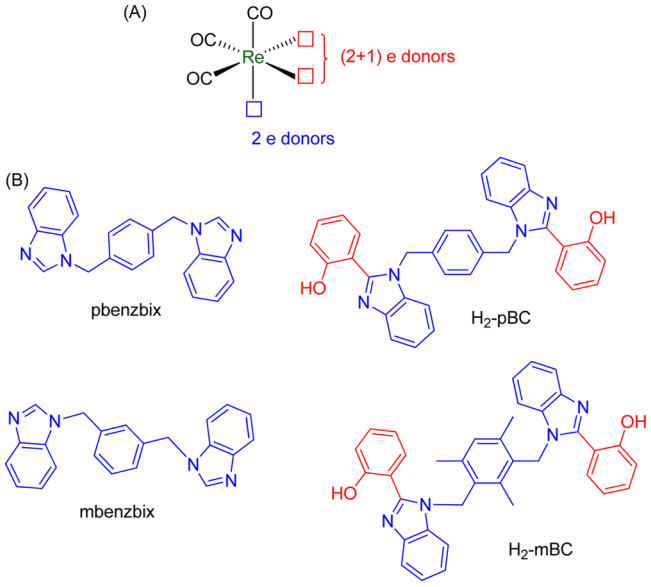

Figure 1. (A) Stereoelectronic requirement of *fac*-$Re(CO)_3$ core. (B) Flexible bis(monodentate) N-donors and flexible bis(bidentate) N∩OH donors.

RESULTS AND DISCUSSION

Synthesis and Characterization of Ligands. Ligand H_2-pBC was synthesized from 2-(2-hydroxyphenyl)-1*H*-benzimidazole (HO-PBH), 1,4-di(bromomethyl)benzene, and NaH in THF (Scheme 1).[7] The isolated ligand is air- and moisture-stable and soluble in polar organic solvents. The ^1H NMR spectrum of H_2-pBC showed well resolved chemical resonances corresponding to the hydroxyphenylbenzimidazolyl (HO-PB) and xylene protons (Supporting Information (SI) Figure S1). The presence of a singlet at 5.36 ppm for the methylene protons, the absence of a NH resonance, and the 1:2 xylene proton to HO-PB units ratio confirmed the formation of the H_2-pBC ligand. A single set of signals was observed for the aromatic and aliphatic protons of H_2-pBC, suggesting the formation of either a single conformer or conformers that undergo rapid conversion in solution on the NMR time scale. The formation of H_2-pBC was further confirmed by ESI-MS, which showed a molecular ion peak at m/z 523.2142 (SI Figure S2).

Scheme 1. Synthesis of H_2-pBC and H_2-mBC Ligands

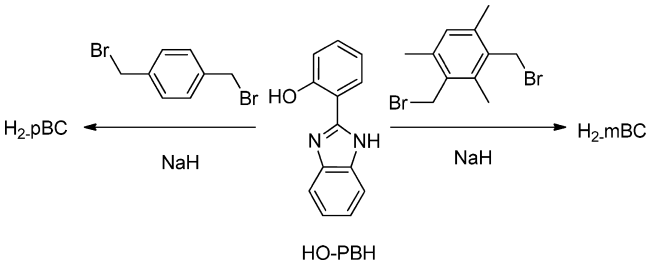

Ligand H_2-mBC was synthesized using the same procedure as that for H_2-pBC (SI Figures S3 and S4). The molecular structures of H_2-pBC and H_2-mBC were optimized using DFT-calculations. Both ligands adopt *anti*-conformation modes in which both the HOPB moieties prefer the intermediate enol structure (Figure 2).

Synthesis and Characterization of Dinuclear Complexes 1−2. Metallocycle **1** was prepared from $Re_2(CO)_{10}$, H_2-pBC, and 1,4-bis(benzimidazol-1-ylmethyl)benzene (pbenzbix) via a one-pot procedure (Scheme 2). The resulting product is air- and moisture-stable, and moderately soluble in polar organic solvents. The FT-IR spectrum of **1** in acetone exhibits strong bands at 2012 (s), 1903 (s), and 1874 (s, br) cm^{-1}, which are characteristic of *fac*-$Re(CO)_3$ in an asymmetric environment (SI Figure S5).[2−5] A similar stretching pattern for the *fac*-$Re(CO)_3$ unit was observed in an acyclic rhenium complex containing *fac*-$Re(CO)_3$ and 2-(1-methyl-1*H*-benzimidazole-2-yl)phenolate with pyridine units in KBr.[8] Complex **2** was synthesized similarly to complex **1** using 1,3-bis(benzimidazol-1-ylmethyl)benzene (mbenzbix) and H_2-mBC in mesitylene. A similar FT-IR pattern was observed for complex **2** (SI Figure S6). The mass analysis revealed a signal that corresponds to a molecular ion at m/z 1401.2047 for $[\mathbf{1}]^+$; 1423.1956 for $[\mathbf{1}+Na]^+$; 1465.2418 for $[\mathbf{2}+Na]^+$; 1481.2153 for $[\mathbf{2}+K]^+$ with an experimental isotope pattern that matches the calculated values (SI Figures S7−S8).

Crystal Structure of Complex 1. Single-crystal X-ray diffraction analysis showed that complex **1** adopts a helicate structure (Figure 3). Each Re(I) ion is surrounded by a N∩O chelating unit (OPB) from the dianionic pBC building unit, a nitrogen atom from pbenzbix, and three carbonyl groups. Thus, complex **1** is best regarded as an unsaturated heterostranded dinuclear double helicate.[9] The two ligand strands wrap around the Re···Re axis in a helical manner. The length of the helix, as defined by the intramolecular Re···Re distance, is 13.01 Å. The twist angle of $(pBC)^{2-}$ in complex **1** is 94° and is defined as the angle between the planes of the two $Re-O_{(Chel)}-N_{(Chel)}$ units.[10]

The helical structure of **1** is further stabilized by intramolecular C−H···π interactions between the two strands (*p*-phenylene unit to *p*-phenylene unit, dihedral angle = 90°, distance = 3.83−4.06 Å). In addition, there are moderate

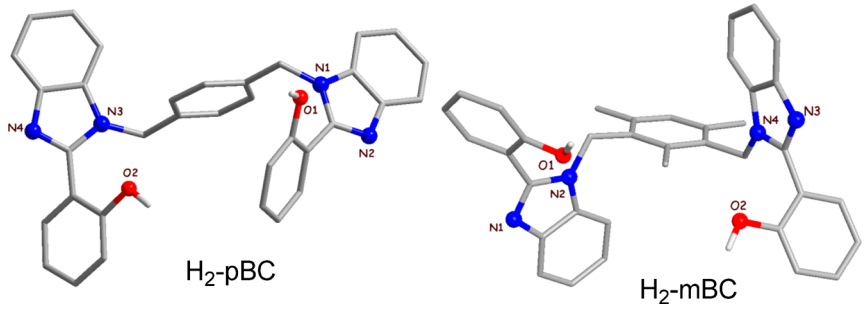

Figure 2. Optimized structures of ligands.

dx.doi.org/10.1021/ic4023135 | *Inorg. Chem.* 2014, 53, 922−930

Scheme 2. Synthesis of Metallocycles 1 and 2

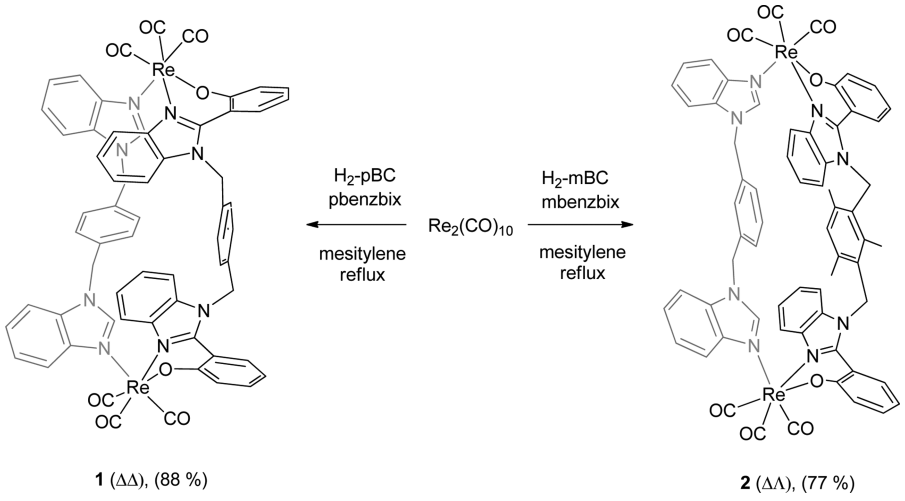

1 (ΔΔ), (88 %) **2** (ΔΛ), (77 %)

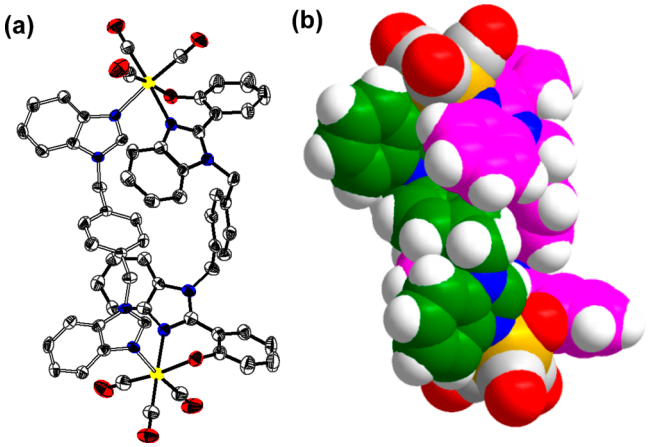

Figure 3. (a) Perspective view of **1** with thermal displacement parameters drawn at 50% probability; hydrogen atoms are omitted for clarity. (b) In the space fill representation, the carbon atoms of the two strands pbenzbix and dianionic pBC are differently colored for clarity. Green = rose = C, white = H, blue = N, red = O, yellow = Re.

intramolecular $\pi\cdots\pi$ stacking interactions between the *p*-phenylene unit of the pbenzbix strand and the two benzimidazolyl units of the pBC strand (dihedral angle = ~22°, centroid-to-edge center distance = 3.7 Å) (SI Figure S9). The $(pBC)^{2-}$ ligand adopts a *syn*-conformation with *anti*-cofacial arrangement of the two OPB units, whereas the pbenzbix adopts an *anti*-conformation with cofacial arrangement of the two benzimidazolyl units in complex **1**. In the crystal packing, each helicate is surrounded by four neighboring helicate molecules that are held together by strong intermolecular $\pi-\pi$ stacking interactions; these intermolecular interactions occur between the same strands, i.e., pbenzbix to pbenzbix and pBC to pBC. Each benzimidazolyl ring is nearly parallel and inverted relative to the benzimidazolyl ring of the adjacent complex; the centroid-to-centroid distance is 3.5 Å (SI Figure S9).

Similar pBC bis-bidendate ligands that contain pyrazolylphenolate coordinating units have been coordinated to naked metal ions to generate homoleptic and heteroleptic double helicates; the resultant complexes are saturated helicates.[11] Large homoleptic helicate molecules have been obtained using benzimidazolyl as coordinating units, and their helical pitches have been calculated and tabulated.[12] To the best of our knowledge, complex **1** is the first neutral dinuclear rhenium-based helicate.[9]

Crystal Structure of Complex 2. Single-crystal X-ray diffraction analysis showed that compound **2** adopts a M_2LL'-type metallomacrocyclic structure (Figure 4 and SI Figure S10).

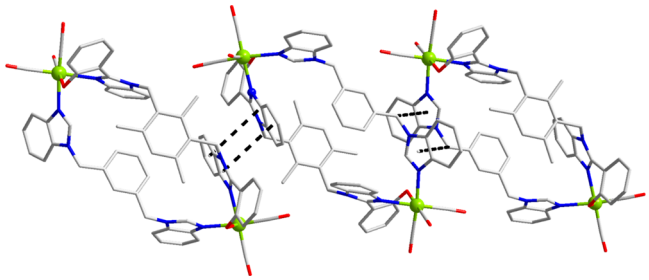

Figure 4. Partial packing diagram of **2** showing a one-dimensional sheet constructed by $\pi\cdots\pi$ stacking interactions. Hydrogen atoms are omitted for clarity.

The molecular structure of **2** is mesohelicate with both ligand strands arranged adjacently. The coordination geometry around the Re centers is a distorted octahedron with a C_3N_2O environment. The dianionic ligand and neutral nitrogen donors adopt a syn-conformation; that is, the two phenolatebenzimidazolyl/two benzimidazolyl units are located on the same sides and serve as "W-type" chelating/bridging units. The Re···Re distance in complex **2** is 13.93 Å, which is 0.9 Å longer than those in helicate **1**; this is expected because the helical nature of the ligand reduces the bridging length of the ligands in complex **1**. The major difference between the two ligands in **2** is the arrangement of the two benzimidazolyl units, which are orientated inward in mBC and outward in mbenzbix with respect to the central phenylene core. Complex **2** features weak intramolecular slipped-cofacial $\pi-\pi$ stacking interactions between the two central phenylene units (SI Figure S10).

In the crystal packing of complex **2**, each molecule interacts with two adjacent molecules that are held together by intermolecular $\pi-\pi$ stacking interactions and CH$-\pi$ interactions (Figure 4). In one direction, weak $\pi-\pi$ stacking interactions occur between the adjacent benzimidazolyl units of the OBP units. In another direction, strong CH$-\pi$ interactions

dx.doi.org/10.1021/ic4023135 | *Inorg. Chem.* 2014, 53, 922−930

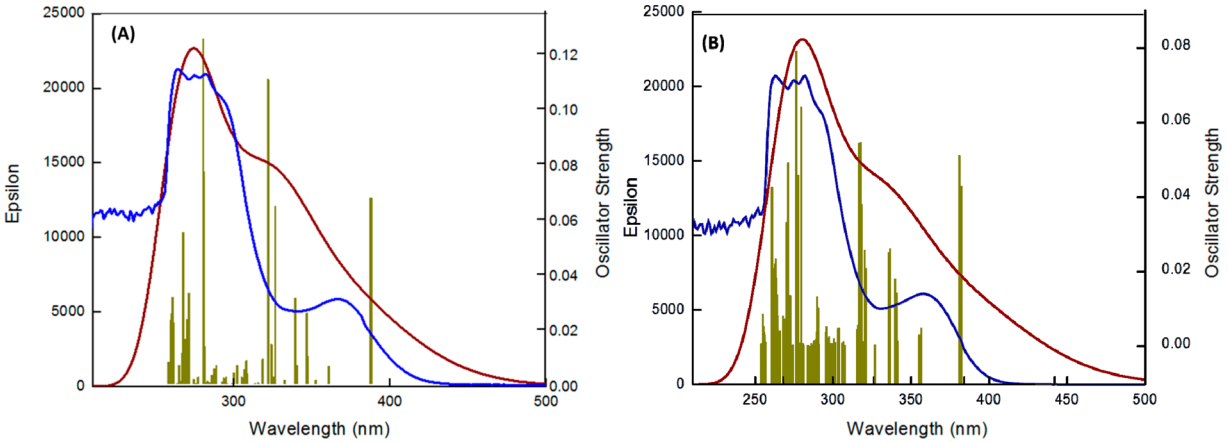

Figure 5. Calculated absorption spectra (maroon) with oscillator strengths (olive) of (A) complex **1** and (B) complex **2**. The blue lines represent the experimental results.

Table 1. Major Absorption Transitions and Corresponding Contributions of Different Molecular Orbitals for Complex 1

absorption transition (nm)	oscillator strength (*f*)	major contributing transitions	character
281	0.1251	HOMO-9 → LUMO (52%),	OPB → pBC (ILCT)
		HOMO-8 → LUMO+1 (−15%)	OPB → OPB ($\pi\pi^*$)
323	0.1105	HOMO-6 → LUMO+1 (30%)	Re,CO → pBC (MLCT)
		HOMO-7 → LUMO (40%)	Re,CO → OPB (MLCT)
327	0.0644	HOMO-2 → LUMO+2 (69%),	Re,CO → p-benzbix (MLCT)
		HOMO-3 → LUMO+3 (−12%)	Re,CO → p-benzbix, pBC (MLCT)
389	0.0675	HOMO-1 → LUMO (55%),	Re,CO, OPB → pBC (MLCT, ILCT)
		HOMO → LUMO+1 (−37%)	Re,CO, OPB → OPB (MLCT)

Table 2. Major Absorption Transitions and Corresponding Contributions of Different Molecular Orbitals for Complex 2

absorption transition (nm)	oscillator strength (*f*)	major contributing transitions	character
276	0.0791	HOMO-9 → LUMO (20%),	OPB → OPB ($\pi\pi^*$)
		HOMO-8 → LUMO+1 (13%),	
		HOMO-1 → LUMO+10 (−11%)	
318	0.0546	HOMO-7 → LUMO (36%),	Re,CO, OPB → (MLCT + ILCT)
		HOMO-7 → LUMO+1 (−16%)	
381	0.051	HOMO-1 → LUMO (−21%),	Re,CO, OPB → OPB (MLCT + ILCT)
		HOMO → LUMO (29%),	
		HOMO → LUMO+1 (43%)	

occur between the methylene units of mbenzbix and the benzimidazolyl units of mbenzbix.

The Re−N bond distances of **1** and **2** are very similar and consistent with values reported for other *fac*-$Re(CO)_3$ complexes containing benzimidazolyl units.[8,13] The $Re-O_{chel}$ and $Re-N_{chel}$ bond lengths are similar to those in previously reported mononuclear complexes, i.e., $[Re(CO)_3(L)$-(pyridine)] (H−L = 2-(1-methyl-1*H*-benzimidazol-2-yl)phenol or 2-(1-phenyl-1*H*-benzimidazole-2-yl)phenol), while the $Re1-N_{(benzimidazolyl)}$ bond length in **1** and **2** is shorter than the $Re-N_{(pyridine)}$ distances (2.217 Å and 2.230 Å) in the mononuclear complexes.

Absorption Spectra. The UV−visible absorption spectra of the Re(I)−carbonyl complexes do not indicate any ground-state aggregation in DMSO within the concentration range of 5×10^{-5} to 10^{-3} M. The absorption spectra of both complexes in DMSO contain strong absorptions between 250 and 300 nm and tail absorbances with band maxima at ∼360 nm (Figure 5 and SI Figure S11). The transitions correspond to $\pi-\pi^*$ transitions, intraligand charge transfer (ILCT), and metal-to-ligand charge transfer (MLCT). To further understand the nature of the different transitions, time-dependent density functional theory (TDDFT) calculations were performed on optimized structures of the complexes. The TDDFT study revealed that the absorption spectra mainly contain three types of intense absorbances at three different regions (Figure 5).

The transition probabilities of the relatively intense transitions of complexes **1** and **2** are compiled in Tables 1 and 2, respectively. The transitions are discussed in detail in the Supporting Information (SI Figures S12−S13).

Emission Spectra. The emission spectra of the complexes were measured both in a nitrogen purged solution and in the presence of air (Figure 6). As in the absorption spectra, the emission spectrum of complex **1** (λ_{max} = 514 nm) is bathochromically shifted from that of complex **2** (λ_{max} = 482 nm), which suggests that the nature of the spacer that interlinks the two OPB moieties affects the spectral characteristics of the complex. The emission spectra are quenched in the presence of air. Interestingly, the spectra in the presence of air are blue-shifted compared to those in the nitrogen-purged solutions. To further elucidate the emission characteristics of the complexes, time-resolved emissions were measured (Table 3 and SI Figure

dx.doi.org/10.1021/ic4023135 | *Inorg. Chem.* 2014, 53, 922−930

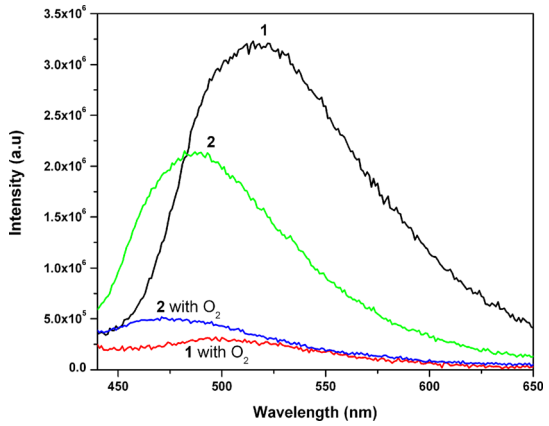

Figure 6. Emission spectra of **1** and **2** in DMSO; λ_{exc} = 365 nm.

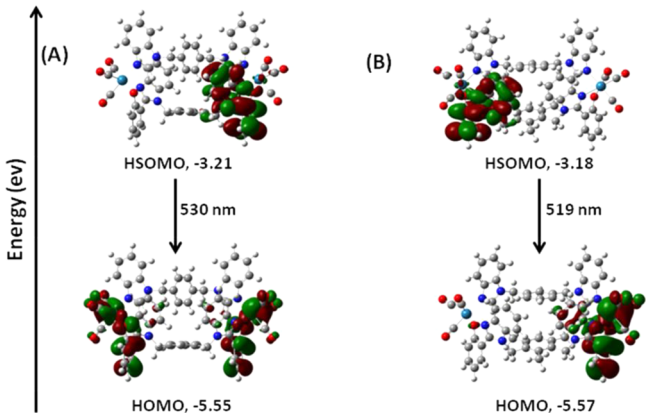

Figure 7. Calculated triplet emission of (A) complex **1** and (B) complex **2**.

S14). The emission decays of both complexes are biexponential in the presence and absence of oxygen. The lifetime of one species is shorter than 1 ns, whereas the other species has a much longer lifetime of a few hundreds of nanoseconds. From the lifetime data, it can be inferred that the complexes emit from two different excited states. The de-excitation of the singlet excited state occurs very fast in the femtosecond time scale, and longer emission occurs from the triplet state in the rhenium complexes.[14] Therefore, the long lifetime component in the emission of **1** and **2** can be assigned to the ^{3}MLCT state. The calculated triplet emission energies further substantiate the conclusion (Figure 7). The highest single occupied molecular orbital (HSOMO) is mainly localized on the OPB ring of the ligand center (95%) in both complexes **1** and **2**. The short lifetime component is due to the fluorescence of the ligand. Similar dual emission due to superimposition of fluorescence of ligand upon long-lived ^{3}MLCT phosphorescence was observed in other rhenium complexes.[15] As expected, the phosphorescence, which occurs at longer wavelengths, is quenched by oxygen more than the fluorescence. Accordingly, the emission spectra of the complexes are blue-shifted in the presence of oxygen.

Solid-State Luminescence. The emission spectra of the solid-state complexes (Figure 8) red-shifted compared to those in solution; this observation clearly contradicts the hypsochromic shift that generally occurs due to rigidochromism in the solid state.[16] Time-resolved emissions of the Re(I) complexes clearly indicate that the complexes also exhibit dual emission in the solid state (Table 4). However, no short-lived fluorescence emission was detected during the luminescence decay measurements. The lifetimes of both emitting states are longer than the phosphorescence of complexes in solution. XRD diffraction studies unambiguously established the aggregation of the complexes due to intermolecular $\pi-\pi$ interactions and CH$-\pi$ interactions between two adjacent metallocycles (Figure 4 and SI Figure S9). In solid-state excitation spectra, a new band is observed at ~420 nm along with a band at 365 nm (SI Figure

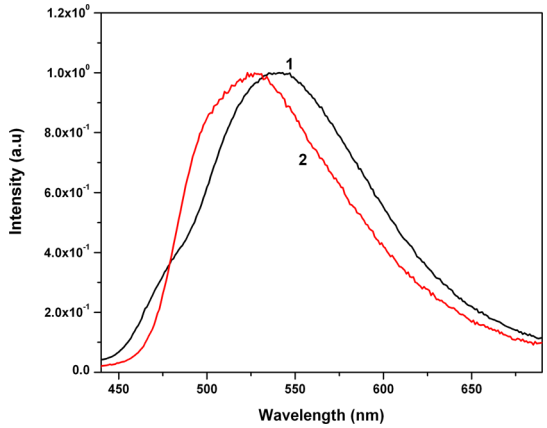

Figure 8. Emission spectra of complexes **1** and **2** in solid state (λ_{exc} = 424 nm).

Table 4. Excited State Lifetimes (τ, ns) of the Complexes in Solid State

	$\lambda_{mon}{}^a$	τ_1	τ_2	χ^2
complex **1**	540	800 (15%)	11000 (85%)	1.02
complex **2**	530	600 (26%)	2800 (74%)	1.04

$^a\lambda_{mon}$ = monitoring wavelength (nm).

S15). The additional excitation band substantiates the aggregation of the complex in the solid state. Additional phosphorescence is also observed in the solid state as a result of this aggregation.

Aggregation-induced phosphorescence has been reported for other metal complexes.[17] In iridium complexes, it has been reported that the energy level of the π^* of the ligand is reduced by $\pi-\pi$ stacking between adjacent ligands, which increases the conjugation.[17a] Therefore, the triplet energy level of the charge-transfer state from the metal to the interacting ligand (denoted

Table 3. Excited State Lifetime (τ, ns) of the Complexes in DMSO

	complex **1**				complex **2**			
	$\lambda_{mon}{}^a$	τ_1	τ_2	χ^2	λ_{mon}	τ_1	τ_2	χ^2
in presence of N_2	514	0.80 (24%)	350 (76%)	1.08	482	1.28 (15%)	176 (84%)	1.09
in presence of air	490	0.70 (40%)	120 (60%)	1.04	470	0.74 (9%)	123 (91%)	1.16

$^a\lambda_{mon}$ - monitoring wavelength (nm).

dx.doi.org/10.1021/ic4023135 | *Inorg. Chem.* 2014, 53, 922−930

as ^{3}MLLCT) decreases and emission occurs from this state in the solid. In the Re complex, aggregation should similarly decrease the energy of the interacting ligand state, resulting in emission from the ^{3}MLCT and ^{3}MLLCT states. Dual emission is a rare phenomenon; however, it has also been observed in some rhenium and iridium complexes.[18]

Electrochemical and Spectroelectrochemical Investigation. The redox properties of the metal complexes were investigated by using cyclic voltammetry. Both **1** and **2** display an oxidation wave in their cyclic voltammogram in CH_2Cl_2/0.1 M Bu_4NPF_6. For complex **1** this process appears at 0.46 V vs ferrocene/ferrocenium and is quasi-reversible (Figure 9). The

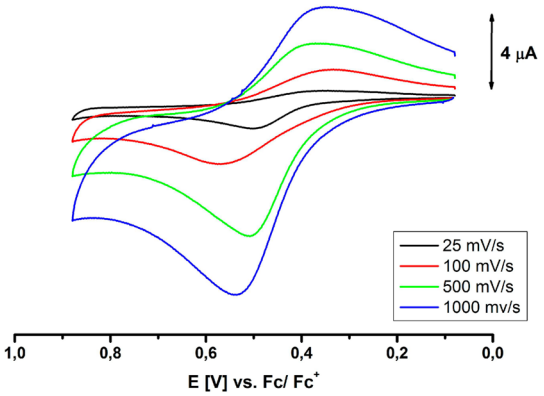

Figure 9. Cyclic voltammograms of **1** in CH_2Cl_2/0.1 M Bu_4NPF_6 with increasing the scan rate of the measurement.

intensity of the reduction peak in the second scan improves by increasing the scan rate of the measurement. For complex **2**, the corresponding redox step appears at comparable potentials. However, the oxidation process is completely irreversible in the case of complex **2**.

To check the reversibility of the redox and determine the site of electron transfer in **1**, IR spectroelectrochemistry was performed on complex **1**. This method can be put to good use to determine reversibility, as seen by the regeneration of the starting spectrum on reversing the redox potential and going back to the initial potential. Furthermore, the presence of the CO markers at the rhenium centers in the complex provides an ideal opportunity to determine the site of electron transfer as observed by the extent of CO shifts on generating the oxidized species. Thus, a rhenium-based oxidation process would shift the starting CO bands by a large extent, since the CO groups are directly attached to the metal centers.[19] On the other hand, an oxidation step taking place predominantly on the bridging ligands would result in only a marginal shift of the CO bands.[20] In CH_2Cl_2, complex **1** shows three strong CO stretching frequencies at 2014, 1904, and 1875 cm^{-1} (SI Figure S16). Upon oxidation of **1**, the CO bands shift to 2038, 2024, and 1933 cm^{-1}; this marginal shift is certainly not compatible with oxidation of the rhenium centers. Hence, the oxidation comprises simultaneous oxidation of the phenoxide moiety of the bridging ligand to generate two spatially separated phenoxyl radicals in the oxidized form of **1**. Simultaneous oxidation of the phenoxide groups is expected because they are symmetrical, spatially well separated, and not conjugated.

The EPR spectrum of the oxidized form of **1** displays a narrow and isotropic signal centered at g = 2.005 at 295 K (Figure 10).[21,22] This confirms the generation of phenoxyl radicals, as proposed from the IR spectroelectrochemistry results, and thus supports a predominantly bridge-centered oxidation of **1**.

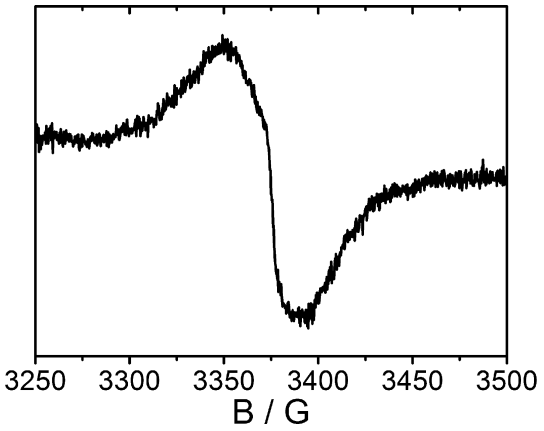

Figure 10. EPR spectrum of oxidized form of **1**.

CONCLUSION

In conclusion, flexible bis(bidentate) N∩OH donors ligand were designed and successfully applied in making a new type of supramolecular architecture. Simultaneous complexation of one flexible bis(monodentate) ligand, one flexible bis(bidentate) unit, and two *fac*-$Re(CO)_3$ cores leads to the self-assembled dinuclear unsaturated double-heterostranded helicate and mesocate. This result may provide the way to develop neutral different shapes and sizes of unsaturated redox active helicates. The complexes emit both fluorescence and phosphorescence in solution. On the other hand, they emit dual phosphorescence due to aggregation-induced structures in the solid state. Our current work is being directed toward changing the *p*-xylene to *o*-xylene and incorporating various functional groups in phenylene and benzimidazolyl units in the ligands and further assembling with *fac*-$Re(CO)_3$ cores.

EXPERIMENTAL SECTION

General Data. Starting materials such as $Re_2(CO)_{10}$, 2-hydroxybenzaldehyde, 1,2-diaminobenzene, 1,4-bis(bromomethyl)-benzene, and NaH (60% dispersion in mineral oil) were procured from commercial sources and used as received. 2-(2-Hydroxyphenyl)-1*H*-benzimidazole (HO-PBH),[23] 1,3-di(bromomethyl)-2,4,6-trimethylbenzene,[24] pbenzbix, and mbenzbix[25] were synthesized by previously reported methods. Elemental analyses were performed on a Elementar Analysensysteme GmbH Vario EL-III instrument. FT-IR spectra were recorded on a Perkin-Elmer FTIR-2000 spectrometer. ^{1}H NMR spectra were recorded on Jeol JNMECX-400P and Bruker AMX-400 FT-NMR spectrometers. A Lambda 35 UV/visible spectrophotometer from PerkinElmer was used to record the absorption spectra. The mass spectra were performed on a Bruker MaXis Impact ESI mass spectrometer. Fluorescence spectra were measured on a Horiba Jobin Yovon Fluoromax4 fluorimeter. Time-resolved fluorescence were measured by the time correlated single photon counting method using an Edinburg Instruments Life Spec II instrument. A picosecond 375 nm laser diode was used as a light source. The full width of half maxima of the laser diode is 90 ps. EPR spectra in the X-band were recorded with a Bruker System EMX. IR spectra were obtained using a Nicolet 6700 FTIR instrument. Cyclic voltammetry was carried out in 0.1 M Bu_4NPF_6 solutions using a three-electrode configuration (glassy-carbon working electrode, Pt counter electrode, Ag wire as pseudoreference), and a PAR 273 potentiostat and function generator. The ferrocene/ferrocenium (Fc/Fc^+) couple served as internal reference. Spectroelectrochemistry was

dx.doi.org/10.1021/ic4023135 | *Inorg. Chem.* 2014, 53, 922−930

performed using an optically transparent thin-layer electrode (OTTLE) cell.[26]

Synthesis of 1,4-Bis(2-(2-hydroxyphenyl)benzimidazol-1-ylmethyl)benzene (H_2-pBC). A mixture of NaH (1.0731 g, 0.0268 mol) and 2-(2-hydroxyphenyl)benzimidazole (2.1235 g, 0.01 mol) in THF (40 mL) was placed in a round-bottom flask and was allowed to stir for 2 h at 45 °C. Solid 1,4-di(bromomethyl)benzene (1.3305 g, 0.005 mol) was then added to the reaction mixture, which was allowed to stir continuously for 4 days at 45 °C. The solvent was removed under reduced pressure. The residue was poured into 100 mL of water. The solid was extracted from the water solution using chloroform, and the organic layer was dried over anhydrous sodium sulfate. The ligand was obtained by removing the solvent under reduced pressure. Yield: 21% (0.626 g). ^{1}H NMR (400 MHz, DMSO-d_6): 7.66 (d, 2H, J = 7.44 Hz, H^4), 7.36−7.30 (m, 6H, $H^{6,3',5'}$), 7.22−7.14 (m, 4H, $H^{5,6'}$), 6.99 (d, 2H, J = 7.32 Hz, H^7), 6.88 (s, 4H, H^9, p-phenylene), 6.87−6.82 (m, 2H, $H^{4'}$), and 5.36 (s, 4H, H^8). ^{13}C NMR (100.5 MHz, DMSO-d_6): 156.05, 151.9, 142.2, 136.07, 134.98, 131.48, 130.85, 126.88, 122.51, 122.01, 119.2, 118.86, 116.5, 116.32, 110.88, and 47.22 (CH_2). ESI-MS: $[M]^+$ for 523.2142 and $[M+Na]^+$ for 545.1961 Anal. Calcd for $C_{34}H_{26}N_4O_2{\cdot}C_4H_8O$: C, 76.75; H, 5.76; N, 9.42. Found: C, 76.95; H, 5.48; N, 9.64.

Synthesis of 1,3-Bis(2-(2-hydroxyphenyl)benzimidazol-1-ylmethyl)-2,4,6-trimethylbenzene (H_2-mBC). The ligand H_2-mBC was obtained by following the same procedure for **1** using NaH (2.0465 g, 0.0512 mol), 2-(2-hydroxyphenyl)benzimidazole (4.2115 g, 0.02 mol), and 1,3-di(bromomethyl)-2,4,6-trimethylbenzene (3.0762 g, 0.01 mol) in THF (40 mL). Yield: 73% (4.301 g). ^{1}H NMR (400 MHz, DMSO-d_6): 10.42 (s, 2H, OH), 7.59 (d, 2H, J = 8.08 Hz, H^4), 7.42 (dd, 2H, J = 8.04 Hz, $H^{3'}$), 7.34−7.39 (m, 2H, $H^{5'}$), 7.1 (t, 2H, J = 7.32 Hz, H^5), 7.01 (d, 2H, J = 8.08 Hz, $H^{6'}$), 6.94 (t, 2H, J = 7.34 Hz, $H^{4'}$), 6.9 (s, 1H, H^9), 6.85 (t, 2H, J = 7.7 Hz, H^6), 6.50 (d, 2H, J = 8.76 Hz, H^7), 5.28 (s, 4H, H^8), 2.04 (s, 6H, H^{11}), and 1.74 (s, 3H, H^{10}). ^{13}C NMR (100.5 MHz, DMSO-d_6): δ 156.15, 152.57, 142.59, 137.31, 134.3, 131.41, 131.34, 130.93, 130.17, 122.09, 121.32, 119.19, 118.97, 117.45, 116.06, 110.84, 44.75 (CH_2), 19.85 (CH_3) and 15.33 (CH_3). ESI-MS: $[M]^+$ for 565.2697 and $[M+Na]^+$ for 587.2530. Anal. Calcd for $C_{37}H_{32}N_4O_2{\cdot}H_2O$: C, 76.27; H, 5.88; N, 9.62. Found: C, 76.44; H, 5.5; N, 9.44.

Synthesis of [($Re(CO)_3)_2$(pBC)(pbenzbix)] (1). A mixture of $Re_2(CO)_{10}$ (100.3 mg, 0.1537 mmol), H_2-pBC·C_4H_8O (80.1 mg, 0.1346 mmol), and pbenzbix (51.9 mg, 0.1533 mmol) in mesitylene (25 mL) was refluxed for 7 h. Yellow product was filtrated at hot conditions and was washed with distilled mesitylene. Yield: 88% (188.7 mg). ESI-MS $[M]^+$ for 1401.2047 and $[M+Na]^+$ for 1423.1956. Crystals obtained from toluene: Anal. Calcd for $C_{62}H_{42}N_8O_8Re_2{\cdot}C_7H_8$: C, 55.56; H, 3.38; N, 7.51. Found: C, 55.33; H, 3.18; N, 7.83.

Synthesis of [($Re(CO)_3)_2$(mBC)(mbenzbix)] (2). A mixture of $Re_2(CO)_{10}$ (100.7 mg, 0.1543 mmol), mbenzbix (52.0 mg, 0.1536 mmol), and H_2-mBC·H_2O (86.6 mg, 0.1486 mmol) in mesitylene (25 mL) was refluxed for 10 h. Yellow precipitate was obtained. The powder was separated by filtration at hot conditions and washed with distilled mesitylene. Yield: 77% (172.1 mg). ESI-MS: $[M+Na]^+$ for 1465.2418 and $[M+K]^+$ for 1481.2153. Crystals obtained from toluene: Anal. Calcd for $C_{65}H_{48}N_8O_8Re_2{\cdot}0.5C_7H_8$: C, 55.31; H, 3.52; N, 7.53. Found: C, 55.04; H, 3.64; N, 7.15.

X-ray Crystallography. A single crystal X-ray structural study of **1** and **2** was performed on an Oxford Diffraction X caliber Sapphire 3 diffractometer equipped with a low-temperature attachment. Data were collected at low temperature using graphite-monochromator Mo Kα radiation (λ_α = 0.71073 Å). The strategy for the data collection was evaluated by using the *CrysAlis PRO* software. The data were collected by the standard phi-omega scan techniques and were scaled and reduced using *CrysAlis RED* software.[27] The structure was solved by direct methods using SHELXS-97 and refined by full matrix least-squares with SHELXL-97, refining on F^2. The positions of all the atoms were obtained by direct methods. All non-hydrogen atoms were refined anisotropically. The remaining hydrogen atoms were placed in geometrically constrained positions and refined with isotropic temperature factors.

Computational Section. The geometry optimizations of H_2-pBC and H_2-mBC were carried out in the gas phase using the B3LYP method with the 6-311+G(d,p) basis set. The initial geometry was obtained from the X-ray crystal structure coordinates of **1** and **2**. The singlet ground state geometry optimizations of **1** and **2** were carried out in the gas phase using the B3LYP method. A Stuttgart−Dresden (SDD) basis set with an effective core potential was used for the rhenium atom. The 6-311G* basis set was used for all other atoms except rhenium, using the Gaussian 03 program package.[28−31] The triplet state geometry optimizations of **1** and **2** were carried out in the gas phase using the UB3LYP method. Geometry optimizations were attained without any constraints. To exactly inspect the absorption spectra, UV−visible spectral analysis for vertical excitations from the ground state was computed using the time dependent density functional theory (TDDFT) in the gas phase. The TDDFT calculation was performed, and the B3LYP functional and SDD/6-311G* basis set for **1** and **2** were used in the optimization step. A total of the lowest 100 singlet excited states and their corresponding oscillator strengths were determined using a TDDFT calculation for **1** and **2**. The Chemissian and GaussSum programs were used to calculate the percentage contribution of various groups and the electronic spectral simulation. The predicted emission wavelengths were obtained by energy differences between the triplet and singlet optimized states.

■ ASSOCIATED CONTENT

Ⓢ Supporting Information

Spectral data of ligands, **1**, and **2** and selected molecular orbitals of **1** and **2**. X-ray crystallographic data for **1** and **2** in CIF format. This material is available free of charge via the Internet at http://pubs.acs.org.

■ AUTHOR INFORMATION

Corresponding Author

*E-mail: msathi@chemistry.du.ac.in; mvdiran@yahoo.com.

Notes

The authors declare no competing financial interest.

■ ACKNOWLEDGMENTS

We thank CSIR, New Delhi, and USIC, University of Delhi, for financial support and the instrument facility. The authors thank the central instruments facility (CIF), IIT Guwahati, for the Life Spec II instrument. We thank Dr. A. Thamaraichelvan, Thiagarajar College, Madurai, for his continuous research support.

■ REFERENCES

(1) (a) Lehn, J. M. *Angew. Chem. Int., Ed.* **2013**, *52*, 2836. (b) Cook, T. R.; Zheng, Y. R.; Stang, P. J. *Chem. Rev.* **2013**, *113*, 734. (c) Inokuma, Y.; Kawano, M.; Fujita, M. *Nat. Chem.* **2011**, *3*, 349. (d) Wiester, M. J.; Ulmann, P. A.; Mirkin, C. A. *Angew. Chem., Int. Ed.* **2011**, *50*, 114. (e) Wang, Z. J.; Clary, K. N.; Bergman, R. G.; Raymond, K. N.; Dean Toste, F. *Nat. Chem.* **2013**, *5*, 100. (f) Smulders, M. M. J.; Riddell, I. A.; Browne, C.; Nitschke, J. R. *Chem. Soc. Rev.* **2013**, *42*, 1728. (g) Saalfrank, R. W.; Maid, H.; Scheurer, A. *Angew. Chem., Int. Ed.* **2008**, *47*, 8794. (h) Hiratani, K.; Albrecht, M. *Chem. Soc. Rev.* **2008**, *37*, 2413. (i) Ward, M. D. *Chem. Commun.* **2009**, 4487. (j) Han, Y. F.; Li, H.; Jin, G. X. *Chem. Commun.* **2010**, *46*, 6879. (k) Saha, M. L.; De, S.; Pramanik, S.; Schmittel, M. *Chem. Soc. Rev.* **2013**, *42*, 6860. (l) Frischmann, P. D.; MacLachlan, M. J. *Chem. Soc. Rev.* **2013**, *42*, 871. (m) Lippert, B.; Miguel, P. J. S. *Chem. Soc. Rev.* **2011**, *40*, 4475. (n) Sauvage, J. P.; Amabilino, D. B. *Top. Curr. Chem.* **2012**, *323*, 107. (o) Therrien, B. *Top. Curr. Chem.* **2012**, *319*, 35. (p) Zangrando, E.; Casanova, M.; Alessio, E. *Chem. Rev.* **2008**, *108*, 4979. (q) Chifotides, H. T.; Dunbar, K. R. *Acc. Chem. Res.* **2013**, *46*, 894. (r) Yam, V. W. W.; Wong, K. M. C. *Chem. Commun.* **2011**, *47*, 11579. (s) Safont-Semere, M. M.; Fernandez, G.; Wurthner, F. *Chem.*

Rev. **2011**, *111*, 5784. (t) Lim, S. H.; Su, Y.; Cohen, S. M. *Angew. Chem., Int. Ed.* **2012**, *51*, 5106. (u) Cook, T. R.; Vajpayee, V.; Lee, M. H.; Stang, P. S.; Chi, K. W. *Acc. Chem. Res.* **2013**, *46*, 2464. (v) Amouri, H.; Desmarets, C.; Moussa, J. *Chem. Rev.* **2012**, *112*, 2015.
(2) (a) Dinolfo, P. H.; Hupp, J. T. *Chem. Mater.* **2001**, *13*, 3113. (b) Kumar, A.; Sun, S. S. Photophysics and Photochemistry of Molecular Recognition and Sensing with Metal-Directed Macrocyclic Systems. In *Molecular Self-Assembly: Advances and Applications*; DequanA. L., Ed.; Pan Stanford Publishing: 2012; p 301. (c) Thanasekaran, P.; Lee, C. C.; Lu, K. L. *Acc. Chem. Res.* **2012**, *45*, 1403. (d) Thorp-Greenwood, F. L.; Balasingham, R. G.; Coogan, M. P. *J. Organomet. Chem.* **2012**, *714*, 12.
(3) (a) Dinolfo, P. H.; Coropceanu, V.; Bredas, J. L.; Hupp, J. T. *J. Am. Chem. Soc.* **2006**, *128*, 12592. (b) Dinolfo, P. H.; Williams, M. E.; Stern, C. L.; Hupp, J. T. *J. Am. Chem. Soc.* **2004**, *126*, 12989. (c) Dinolfo, P. H.; Hupp, J. T. *J. Am. Chem. Soc.* **2004**, *126*, 16814. (d) Keefe, M. H.; O'Donnell, J. L.; Bailey, R. C.; Nguyen, S. T.; Hupp, J. T. *Adv. Mater.* **2003**, *15*, 1936. (e) Mines, G. A.; Tzeng, B. C.; Stevenson, K. J.; Li, J.; Hupp, J. T. *Angew. Chem., Int. Ed.* **2002**, *41*, 154. (f) Williams, M. E.; Benkstein, K. D.; Abel, C.; Dinolfo, P. H.; Hupp, J. T. *Proc. Natl. Acad. Sci. U.S.A.* **2002**, *99*, 5171. (g) Merlau, M. L.; del Pilar Mejia, M.; Nguyen, S. T.; Hupp, J. T. *Angew. Chem., Int. Ed.* **2001**, *40*, 4239.
(4) (a) Botana, E.; Silva, E. D; Benet-Buchholz, J.; Ballester, P.; de Mendoza, J. *Angew. Chem., Int. Ed.* **2007**, *46*, 198. (b) Orsa, D. K.; Haynes, G. K.; Pramanik, S. K.; Iwunze, M. O.; Greco, G. E.; Krause, J. A.; Ho, D. M.; Williams, A. L.; Hill, D. A.; Mandal, S. K. *Inorg. Chem. Commun.* **2007**, *10*, 821.
(5) (a) Shankar, B.; Elumalai, P.; Shanmugam, R.; Sathiyendiran, M. *J. Organomet. Chem.* **2014**, *749*, 224. (b) Shankar, B.; Elumalai, P.; Shanmugam, R.; Singh, V.; Masram, D. T.; Sathiyendiran, M. *Inorg. Chem.* **2013**, *52*, 10217−10219. (c) Rajakannu, P.; Elumalai, P.; Shankar, B.; Hussain, F.; Sathiyendiran, M. *Dalton Trans.* **2013**, *42*, 11359. (d) Rajakannu, P.; Eumalai, P.; Mobin, M.; Lu, K. L.; Sathiyendiran, M. *J. Organomet. Chem.* **2013**, *743*, 17. (e) Shankar, B.; Elumalai, P.; Jackmil, J.; Kumar, P.; Singh, S.; Sathiyendiran, M. *J. Organomet. Chem.* **2013**, *743*, 109. (f) Shankar, B.; Elumalai, P.; Hussain, F.; Sathiyendiran, M. *J. Organomet. Chem.* **2013**, *732*, 130. (g) Rajakannu, P.; Elumalai, P.; Hussain, F.; Sathiyendiran, M. *J. Organomet. Chem.* **2013**, *725*, 1. (h) Rajakannu, P.; Hussain, F.; Shankar, B.; Sathiyendiran, M. *Inorg. Chem. Commun.* **2012**, *26*, 46. (i) Shankar, B.; Hussain, F.; Sathiyendiran, M. *J. Organomet. Chem.* **2012**, *719*, 26. (j) Gupta, D.; Rajakannu, P.; Shankar, B.; Shanmugam, R.; Hussain, F.; Sarkar, B.; Sathiyendiran, M. *Dalton Trans.* **2011**, *40*, 5433. (k) Rajakannu, P.; Shankar, B.; Yadav, A.; Shanmugam, R.; Gupta, D.; Hussain, F.; Chang, C. H.; Sathiyendiran, M.; Lu, K. L. *Organometallics* **2011**, *30*, 3168. (l) Shankar, B.; Rajakannu, P.; Kumar, S.; Gupta, D.; Kannan, T.; Sathiyendiran, M. *Inorg. Chem. Commun.* **2011**, *14*, 374.
(6) (a) Coogan, M. P.; Moreira, V. F.; Kariuki, B. M.; Pope, S. J. A.; Thorp-Greewood, F. L. *Angew. Chem., Int. Ed.* **2009**, *48*, 4965. (b) Brasey, T.; Buryak, A.; Scopelliti, R.; Severin, K. *Eur. J. Inorg. Chem.* **2004**, 964.
(7) (a) Tewari, A. K.; Mishra, A. *Indian J. Chem.* **2006**, *45B*, 489. (b) Mimassi, L.; Guyard-Duhayon, C.; Raehm, L.; Amouri, H. *Eur. J. Inorg. Chem.* **2002**, 2453. (c) Raehm, L.; Mimassi, L.; Guyard-Duhayon, C.; Amouri, H. *Inorg. Chem.* **2003**, *42*, 5654.
(8) Czerwieniec, R.; Kapturkiewicz, A.; Anulewicz-Ostrowska, R.; Nowacki, J. *J. Chem. Soc., Dalton Trans.* **2002**, 3434.
(9) (a) To our knowledge, the known helical structures based on *fac*-$Re(CO)_3$ core are single-stranded dinuclear helicates. (b) Ho, P. K. K.; Cheung, K. K.; Peng, S. M.; Che, C. M. *J. Chem. Soc., Dalton Trans.* **1996**, 1411. (c) Bardwell, D. A.; Barigelletti, F.; Cleary, R. L.; Flamigni, L.; Guardigli, M.; Jeffery, J. C.; Ward, M. D. *Inorg. Chem.* **1995**, *34*, 2438.
(10) (a) Twist angle of H_2-pBC in **1** is defined as the angle between the plane Re-$O_{(Chel)}$-$N_{(Chel)}$. (b) Domer, J.; Slootweg, J. C.; Hupka, F.; Lammertsma, K.; Hahn, F. E. *Angew. Chem., Int. Ed.* **2010**, *49*, 6430.
(11) (a) Potts, K. T.; Keshavarz-K, M.; Tham, F. S.; Abruna, H. D.; Arana, C. *Inorg. Chem.* **1993**, *32*, 4422. (b) Potts, K. T.; Keshavarz-K, M.; Tham, F. S.; Abruna, H. D.; Arana, C. *Inorg. Chem.* **1993**, *32*, 4436. (c) Ho, P. K. K.; Cheung, K. K.; Che, C. M. *Chem. Commun.* **1996**, 1197.
(12) (a) Xue, Y.-H.; Xua, D-J; Gu, J.-M. *Acta Crystallogr.* **2003**, *C59*, m387−m389. (b) Gschneidner, K., Jr; Bünzli Pecharsky, V. K. *Handbook on the Physics and Chemistry of Rare Earths* **2010**, *40*, 301.
(13) Ju, C. C.; Zhang, A. G.; Sun, H. L.; Wang, K. Z.; Jiang, W. L.; Bian, Z. Q.; Huang, C. H. *Organometallics* **2011**, *30*, 712.
(14) (a) El Nahhas, A.; Consani, C.; Blanco-Rodríguez, A. M.; Lancaster, K. M.; Braem, O.; Cannizzo, A.; Towrie, M.; Clark, I. P.; Záliš, S.; Chergui, M.; Vlček, A. *Inorg. Chem.* **2011**, *50*, 2932. (b) Sato, S.; Matubara, Y.; Koike, K.; Falkenström, M.; Katayama, T.; Ishibashi, Y.; de Miyasaka, H.; Taniguchi, S.; Chosrowjan, H.; Mataga, N.; Fukazawa, N.; Koshihara, S.; Onda, K.; Ishitani, O. *Chem.—Eur. J.* **2012**, *18*, 15722.
(15) Jones, J. E.; Kariuki, B. M.; Ward, B. D.; Pope, S. J. A. *Dalton Trans.* **2011**, *40*, 3498.
(16) (a) Itokazu, K. M.; Polo, S. A.; Iha, M. Y. N. *J. Photochem. Photobio. A* **2003**, *160*, 27. (b) Zhang, L.; Li, B.; Su, Z. *Langmuir* **2009**, *25*, 2068.
(17) (a) Zhao, Q.; Li, L.; Li, F.; Yu, M.; Liu, Z.; Yi, T.; Huang, C. *Chem. Commun.* **2008**, 685. (b) Dai, Q.; Liu, W.; Zeng, L.; Lee, C. S.; Wu, J.; Wang, P. *Cryst. Eng. Comm.* **2011**, *13*, 4617. (c) Moussa, J.; Wong, K. M. C.; Chamoreau, L. M.; Amouri, H.; Yam, V. W. W. *Dalton Trans.* **2007**, 3526. (d) Moussa, J.; Wong, K. M. C.; Goff, X. F.; Le Rager, M. N.; Chan, C. K. M.; Yam, V. W. W.; Amouri, H. *Organometallics* **2013**, *32*, 4985.
(18) (a) Morimoto, T.; Ito, M.; Koike, K.; Kojima, T.; Ozeki, T.; Ishitani, O. *Chem.—Eur. J.* **2012**, *18*, 3292−3304. (b) Yeh, Y. S.; Cheng, Y. M.; Chou, P. T.; Lee, G. H.; Yang, C. H.; Chi, Y.; Shu, C. F.; Wang, C. H. *Chem. Phys. Chem.* **2006**, *7*, 2294. (c) Lo, K. K. W.; Chung, C. K.; Zhu, N. *Chem.—Eur. J.* **2006**, *12*, 1500. (d) Lo, K. K. W.; Zhang, K. Y.; Leung, S. K.; Tang, M. C. *Angew. Chem., Int. Ed.* **2008**, *47*, 2213. (e) Kozhevnikov, D. N.; Kozhevnikov, V. N.; Shafikov, M. Z.; Prokhorov, A. M.; Bruce, D. W.; Gareth Williams, J. A. *Inorg. Chem.* **2011**, *50*, 3804. (f) You, Y.; Han, Y.; Lee, Y. M.; Park, S. Y.; Nam, W.; Lippard, S. J. *J. Am. Chem. Soc.* **2011**, *133*, 11488. (g) You, Y.; Lee, S.; Kim, T.; Ohkubo, K.; Chae, W. S.; Fukuzumi, S.; Jhon, G. J.; Nam, W.; Lippard, S. J. *J. Am. Chem. Soc.* **2011**, *133*, 18328. (h) Ladouceura, S.; Donatoa, L.; Romaina, M.; Mudraboyinab, B. P.; Johansenb, M. B.; Wisnerb, J. A.; Zysman-Colmana, E. *Dalton Trans.* **2013**, *42*, 8838.
(19) Drozdz, A.; Bubrin, M.; Fiedler, J.; Zalis, S.; Kaim, W. *Dalton Trans.* **2012**, *41*, 1013.
(20) Sarkar, B.; Kaim, W.; Schleid, Th.; Hartenbach, I.; Fiedler, J. *Z. Anorg. Allg. Chem.* **2003**, *629*, 1353.
(21) Patra, S.; Sarkar, B.; Mobin, S. M.; Kaim, W.; Lahiri, G. K. *Inorg. Chem.* **2003**, *42*, 6469.
(22) Weisser, F.; Huebner, R.; Schweinfurth, D.; Sarkar, B. *Chem.—Eur. J.* **2011**, *17*, 5727.
(23) Han, X.; Ma, H.; Wang, Y. *Russ. J. Org. Chem.* **2008**, *44*, 872.
(24) van der Made, A. W.; van der Made, R. H. *J. Org. Chem.* **1993**, *58*, 1262.
(25) Su, C. Y.; Cai, Y. P.; Chen, C. L.; Smith, M. D.; Kaim, W.; zur Loye, H. C. *J. Am. Chem. Soc.* **2003**, *125*, 8595.
(26) Krejcik, M.; Danek, M.; Hartl, F. J. *Electroanal. Chem. Interfacial Electrochem.* **1991**, *317*, 179.
(27) (a) Oxford Diffraction (2009). *CrysAlis PRO and CrysAlis RED.*: Oxford Diffraction Ltd, Yarnton, England. (b) Sheldrick, G. M. *Acta Crystallogr.* **2008**, *A64*, 112.
(28) (a) Becke, A. D. *J. Chem. Phys.* **1993**, *98*, 5648. (b) Lee, C.; Yang, W.; Parr, R. G. *Phys. Rev. B* **1988**, *7*, 785. (c) Vosko, S. H.; Wilk, L.; Nusair, M. *Can. J. Phys.* **1980**, *58*, 1200.
(29) (a) McLean, A. D.; Chandler, G. S. *J. Chem. Phys.* **1980**, *72*, 5639. (b) Krishnan, R.; Binkley, J. S.; Seeger, R.; Pople, J. A. *J. Chem. Phys.* **1980**, *72*, 650.

(30) (a) Stratmann, R. E.; Scuseria, G. E.; Frisch, M. J. *J. Chem. Phys.* **1998**, *109*, 8218. (b) Bauernschmitt, R.; Ahlrichs, R. *Chem. Phys. Lett.* **1996**, *256*, 454. (c) Casida, M. E.; Jamorski, C.; Casida, K. C.; Salahub, D. R. *J. Chem. Phys.* **1998**, *108*, 4439.

(31) Frisch, M. J.; Trucks, G. W.; Schlegel, H. B.; Scuseria, G. E.; Robb, M. A.; Cheeseman, J. R.; Montgomery, J. A. Jr.; Vreven, T.; Kudin, K. N.; Burant, J. C.; Millam, J. M.; Iyengar, S. S.; Tomasi, J.; Barone, V.; Mennucci, B.; Cossi, M.; Scalmani, G.;ega, N.; Petersson, G. A.; Nakatsuji, H.; Hada, M.; Ehara, M.; Toyota, K.; Fukuda, R.; Hasegawa, J.; Ishida, M.; Nakajima, T.; Honda, Y.; Kitao, O.; Nakai, H.; Klene, M.; Li, X.; Knox, J. E.; Hratchian, H. P.; Cross, J. B.; Bakken, V.; Adamo, C.; Jaramillo, J.; Gomperts, R.; Stratmann, R. E.; Yazyev, O.; Austin, A. J.; Cammi,R.; Pomelli, C.; Ochterski, J. W.; Ayala, P. Y.; Morokuma, K.; Voth, G. A.; Salvador, P.; Dannenberg, J. J.; Zakrzewski, V. G.; Dapprich, S.; Daniels, A. D.; Strain, M. C.; Farkas, O.; Malick, D. K.; Rabuck, A. D.; Raghavachari, K.; Foresman, J. B.; Ortiz, J. V.; Cui, Q.; Baboul, A. G.; Clifford, S.; Cioslowski, J.; Stefanov, B. B.; Liu, G.; Liashenko, A.; Piskorz, P.; Komaromi, I.; Martin, R. L.; Fox, D. J.; Keith, T.; Al-Laham, M. A.; Peng, C. Y.; Nanayakkara, A.; Challacombe, M.; Gill, P. M. W.; Johnson, B.; Chen, W.; Wong, M. W.; Gonzalez, C.; Pople, J. A. Gaussian 03, revision E.01; Gaussian, Inc.: Wallingford, CT, 2003.